Breast Tissue Chemistry Measured In Vivo In Healthy Women Correlate with Breast Density and Breast Cancer Risk

Gorane Santamaría, MD, PhD,[1,2,3,4*] Natali Naude, BAppSc, PhD,[1,2,4] Julia Watson, BAppSc (MRT),[1,2,4] John Irvine, PhD,[4] Thomas Lloyd, MD,[2,4] Ian Bennett, MD,[2] Graham Galloway, PhD,[1,2,4] Peter Malycha, MD,[1,2,4,5] and Carolyn Mountford, DPhil, MS[1,2,4]

Background: The relationship of tissue chemistry to breast density and cancer risk has not been documented despite breast density being a known risk factor.
Purpose: To investigate whether distinct chemical profiles associated with breast density and cancer risk are identified in healthy breast tissue using in vivo two-dimensional correlated spectroscopy (2D COSY).
Study Type: Prospective.
Population: One-hundred-seven participants including 55 at low risk and 52 at high risk of developing breast cancer.
Field Strength/Sequence: 3 T/ axial/ T1, T2, 2D COSY.
Assessment: Two radiologists defined breast density on T2. Interobserver variability assessed. Peak volumes normalized to methylene at (1.30, 1.30) ppm as internal shift reference.
Statistical Tests: Chi-squared/Mann–Whitney/*Kappa* statistics/Kruskal Wallis/pairwise analyses. Significance level 0.05.
Results: Ten percentage were fatty breasts, 39% scattered fibroglandular, 35% heterogeneously dense, and 16% extremely dense. Interobserver variability was excellent (*kappa* = 0.817). Sixty percentage (64/107) were premenopausal. Four distinct tissue chemistry categories were identified: low-density (LD)/premenopausal, high-density (HD)/premenopausal, LD/postmenopausal, and HD/postmenopausal. Compared to LD, HD breast chemistry showed significant increases of cholesterol (235%) and lipid unsaturation (33%).
In the low-risk category, postmenopausal women with dense breasts recorded the largest significant changes including cholesterol methyl 540%, lipid unsaturation 207%, glutamine/glutamate 900%, and choline/phosphocholine 800%.
In the high-risk cohort, premenopausal women with HD recorded a more active chemical profile with significant increases in choline/phosphocholine 1100%, taurine/glucose 550% and cholesterol sterol 250%.
Data Conclusion: Four distinct chemical profiles were identified in healthy breast tissue based on breast density and menopausal status in participants at low and high risk. Gradual increase in neutral lipid content and metabolites was noted in both risk groups across categories in different order. In low risk, the HD postmenopausal category exhibited the highest metabolic activity, while women at high risk exhibited the highest lipid content and metabolic activity in the HD premenopausal category.
Level of Evidence: 2
Technical Efficacy Stage: 3

J. MAGN. RESON. IMAGING 2022;56:1355–1369.

Epidemiological studies report breast density as an independent risk factor for cancer[1–3] with high density (HD) conferring a 4 to 6-fold increased risk of breast cancer.[4] Only age and *BRCA* mutation status are associated with a higher risk.[5] The most widespread method to qualitatively assess breast density is the breast imaging reporting and data

View this article online at wileyonlinelibrary.com. DOI: 10.1002/jmri.28168

Received Apr 7, 2021, Accepted for publication Mar 11, 2022.

*Address reprint requests to: G.S., 199 Ipswich Road, Woolloongabba, QLD 4102, Australia. E-mail: goranes@gmail.com
Gorane Santamaría and Natali Naude are co-first authors

From the [1]Diagnostic Imaging, Translational Research Institute, Woolloongabba, Queensland, Australia; [2]Department of Radiology, Princess Alexandra Hospital, Woolloongabba, Queensland, Australia; [3]Department of Radiology, Hospital Clínic de Barcelona, Barcelona, Spain; [4]Faculty of Health, Biomedical Sciences, Queensland University of Technology, Brisbane, Queensland, Australia; and [5]Jones and Partners Radiology, St Andrew's Hospital, Adelaide, Australia

This is an open access article under the terms of the Creative Commons Attribution-NonCommercial-NoDerivs License, which permits use and distribution in any medium, provided the original work is properly cited, the use is non-commercial and no modifications or adaptations are made.

© 2022 The Authors. *Journal of Magnetic Resonance Imaging* published by Wiley Periodicals LLC on behalf of International Society for Magnetic Resonance in Medicine.

system (BI-RADS) classification.[6] BI-RADS evaluates parenchymal patterns and distributions and classifies the breast density into four categories.[6] Stroma is the major tissue component of the breast and is composed of stromal cells and extracellular matrix proteins.[7] Dense breast tissue contains higher amounts of stroma and less fat than nondense breasts[8] and the increase in breast density is mainly associated with an augmentation in the deposition of collagen.[9]

One-dimensional MR spectroscopy was reported to identify variations in water and lipid ratio of breast tissue related to age, breast density, and menopausal status.[10] A more modern approach using in vivo MR two-dimensional correlated spectroscopy (2D COSY) reported the chemical species unambiguously assigned using a second magnetic frequency.[11,12] This 2D COSY method was used to evaluate breast tissue chemistry in women carrying the *BRCA1* or *BRCA2* gene mutations.[11] Neutral lipid content was reported to differ between the *BRCA1*, *BRCA2*, and healthy cohorts. Recent advances in MR hardware, including magnet stability, coil technology, and the capacity for radiographers to operate the scanner with precision in spectroscopy mode, have resulted in an improved signal-to-noise ratio.

Cell models of tumor development and progression paved the way to evaluate the role of lipid chemistry and metabolism in tumor development and progression. In vitro cell lines were examined and the MR spectral changes were correlated with specific biological and genetic characteristics.[13–15] The earliest biomarkers of the premalignant state(s) were molecules active on the MR timescale and included lipids and cholesterol.[15] In parallel, the causes of the aberrant choline phospholipid metabolism in breast cancer were documented.[16]

Our hypothesis is that the lipid chemistry and metabolites, recorded in well-defined cell models of tumor development and progression, could now be measured in vivo in a clinical scanner and that there is an association between the tissue chemistry, the breast density, and the risk of breast cancer. Therefore, the evaluation of breast tissue chemistry might provide an objective evaluation of both breast density and biomarkers of risk for cancer.

This study aims to investigate whether distinct chemical profiles associated with breast density can be identified in the tissue of healthy women at low and high risk of breast cancer using in vivo 2D COSY.

Material and Methods

Patient Cohort and Inclusion Criteria

Institutional review board approval and written informed consent was obtained from all participants. A cross-sectional study with prospective data collection was carried out between October 2017 and August 2019 at three hospitals. Sixty-four healthy women at low risk and 89 at high risk according to the National Institute for Health and Care Excellence guidelines[17] (Table 1) were consecutively recruited. None of them was pregnant or taking hormone replacement therapy. The lifetime risk was calculated for each patient according to the international breast cancer intervention study (IBIS) score using the Tyrer–Cuzick model[18] (version 8.0b). The American Cancer Society recommends women with a lifetime risk of cancer of 20% or greater as being high risk.[19] According to these guidelines, participants with an IBIS score ≤ 20% were selected from the low-risk cohort. Women with a score > 20% were chosen from the high-risk category. Therefore, the study group included 107 participants (mean age, 44.07 years; SD, 11.48 years; range: 20–72), including 55 at low risk with an IBIS score ≤ 20% and 52 at high risk with no known pathogenic mutations and an IBIS score > 20%.

MR Imaging

Participants underwent MR imaging of the breast and in vivo MR 2D COSY between days 6 and 14 of the menstrual cycle, where relevant. The data were collected on a 3-T Magnetom Prisma or a 3-T Magnetom Vida scanner (Siemens AG, Erlangen, Germany) using either an 18-channel (Siemens AG) or a 16-channel (RAPID Biomedical, Germany) breast coil.

Breast MRI consisted of 1) localizer sequence (repetition time [TR]:6 msec, echo time [TE]: 2.61 msec, slice thickness: 7 mm, field of view [FOV]: 400 x 400 mm^2); 2) axial T1-weighted three-dimensional (3D) flash (TR: 5.43 msec, TE: 2.46 msec, flip angle: 20°, slice thickness: 2 mm, FOV: 320 x 320 mm^2, matrix: 448 × 448 mm^2); and 3) axial T2-weighted TSE sequence (TR: 4280 msec, TE: 97 msec, slice thickness: 2 mm, FOV: 300 x 300 mm^2, matrix: 448 × 448 mm^2).

A dynamic axial 3D fat suppressed T1-weighted gradient-echo sequence was added to the protocol in women at high risk (TR: 4.51 msec; TE: 2.03 msec; flip angle: 10°; slice thickness: 1.2 mm; FOV: 320 × 320 mm^2; matrix: 448 × 448 mm^2; in-plane resolution: 0.7 × 0.7 mm^2, acquisition time 91.5 seconds). Images were obtained prior to a rapid bolus injection and five times after injection of contrast material, with a resulting total imaging time of 9 minutes 9 seconds. The bolus injection consisted of 0.1-mmol gadobutrol (Gadovist; Bayer, Berlin, Germany) per kilogram of body weight and a 20-mL saline flush, delivered through an intravenous cannula. Automated subtraction of the appropriate precontrast and postcontrast images and multiplanar reconstruction of data sets were performed.

Using the T2-weighted sequence, two radiologists (G.S. and T. L.) with 20 years and 10 years of experience in breast imaging independently assessed the breast density based on BI-RADS classification[6]: category a (fatty breast), category b (scattered density), category c (heterogeneous density), and category d (extremely dense breast). For analysis purposes, a

TABLE 1. Family Risk Assessment Participant Selection Protocol According to the National Institute for Health and Care Excellence Guidelines[17]

Low Risk	Medium Risk	High Risk
No family history of breast cancer One first-degree relative with breast cancer >40 One second-degree relative with breast cancer at any age Two first- or second-degree relatives with breast cancer >50 (on different sides of the family)	One first-degree relative with breast cancer <40 Two first- or second-degree relatives with breast cancer at an average age > 50 Three first- or second-degree relatives with breast cancer at an average age > 60	Two first- or second-degree relatives with breast cancer <50 Three first- or second-degree relatives with breast cancer <60 Four relatives with breast cancer at any age Two first- or second-degree relatives with breast or ovarian cancer plus any of the following: 1. Additional relative with breast or ovarian cancer 2. Breast cancer diagnosed <40 3. Ovarian cancer diagnosed <50 4. Bilateral breast cancer 5. Breast and ovarian cancer in the same woman 6. Ashkenazi Jewish Ancestry 7. Breast cancer in a male relative 8. First- or second-degree relative diagnosed with sarcoma ≤45 One member of a family where a breast cancer gene has been identified

and b made up the low-density (LD) group, whereas c and d made up the HD group. Interobserver variability was assessed. For discrepancies in assessing the amount of fibroglandular tissue (low vs. high), the radiologists agreed on the breast density type that would be recorded for further analysis.

Two-Dimensional Correlated Spectroscopy

A 3D T1-weighted sequence was used to position a voxel of $20 \times 20 \times 20$ mm^3 in the left breast. To get a reliable description of the breast tissue chemistry related to a specific category of breast density, the voxel was placed in a region that mainly included fatty tissue whenever the overall breast density was type a; a mixture of fat and fibroglandular tissue in participants with type b or type c (predominantly fat in type b and fibroglandular tissue in type c) and fibroglandular tissue in those participants with type d (Fig. 1).

Localized shimming was performed using the automatic B0-field mapping technique Siemens auto-shimming algorithm,[20] followed by manual adjustment of zero order shim gradients to achieve a width of the water peak at half maximum of ≤65 Hz.

The 2D COSY sequence parameters were TR of 2000 msec, TE initial of 30 msec, 96 t1 increments at 0.8 msec, 6 averages per increment, f2 bandwidth of 2000 Hz, vector size of 1024 points, and RF offset frequency set on 3.2 ppm. "WET" water suppression[21] was applied. The total acquisition time was 19 minutes. Processing was undertaken as reported by Ramadan[11] and participants were instructed to remain still.

For the measurement of cross peak and diagonal peak volumes, all peak volumes were normalized to the methylene peak at (1.30, 1.30) ppm as the internal chemical shift reference. Next, a box was prescribed on top of each peak, and lastly, the Felix 2D/ND software (Felix NMR, San Diego, California, USA) was used for off-line data processing, spectral visualization, and analysis of high-resolution NMR data measuring the volume of signal under these boxes. Peak assignments were noted along (F2, F1) in ppm and made as previously reported by Ramadan and Thomas in vivo[11,12] and by Sitter et al from breast tissue extracts.[22]

Standard spectral analysis utilized a level multiplier of 1.4, whereas for metabolite regions, we utilized a level multiplier of 1.05 to make it possible identify the diagonal peaks of metabolites.

Statistical Analysis

Statistical analysis was undertaken using IBM SPSS Statistics 25.0 (IBM, Armonk, New York, USA). Age, MRI BI-RADS category of breast density, menopausal status, body mass index (BMI), IBIS risk score, measured volume of various lipid diagonal peaks and cross peaks, metabolites, and cholesterol were collected for each participant.

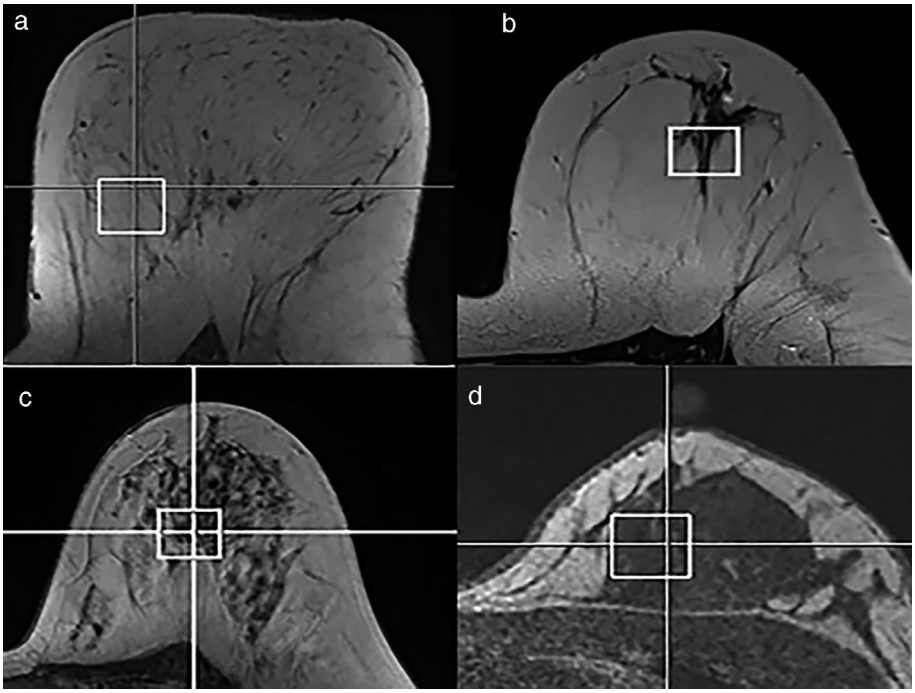

FIGURE 1: T2-weighted sequence. Voxel placement according to different breast density (a, b, c, or d) for the spectra to reflect the overall breast density. (a) Fatty breast, (b) scattered fibroglandular tissue, (c) heterogeneously dense breast, and (d) extremely dense breast.

Chi-squared test was used to compare categorical variables. Mean comparison between low- and high-risk groups of developing breast cancer and between low and high breast density categories was performed using Mann–Whitney test. Interobserver variability was assessed by *kappa* statistics for qualitative data. Kruskal–Wallis test was used for mean comparison across several categories and Bonferroni correction for pairwise comparison of the means. A two-sided *P*-value of <0.05 was considered statistically significant.

Results

Clinical Features

The demographics of the cohort are listed in Table 2. No significant differences in age ($P = 0.632$), menopausal status ($P = 0.221$), or BMI ($P = 0.622$) were recorded between the low- and high-risk groups. Sixty percentage (64/107) of participants were premenopausal and the remaining 40% (43/107) postmenopausal.

The breast density distribution in this cohort was made up of 10% (11/107) type a, 39% (42/107) type b, 35% (37/107) type c, and 16% (17/107) type d. LD and HD categories included 53 and 54 participants, respectively. A significantly higher proportion of LD breasts was noted in the low-risk cohort in comparison with the high-risk group. The interobserver variability for the breast density assessment in terms of LD or HD was excellent (*kappa* coefficient = 0.817).

In Vivo 2D COSY of Healthy Human Breast Tissue

The improved capability of the 3-T scanners used in this study has resulted in new assignments. A representative 2D COSY spectrum of the region F2/F1: 0.00 ppm to 6.00 ppm, with the cross peaks assigned (A–G′), is shown for an HD/postmenopausal participant in Fig. 2a. The triglyceride molecule, with associated cross peaks labeled (A–G′), can be seen in Fig. 2b. The spin–spin coupling between adjacent hydrogen atoms are denoted. The G′ is seen in Fig. 2a as two clear cross peaks not previously reported in vivo in the human breast.

Typical spectra recorded from LD/premenopausal, LD/postmenopausal, HD/premenopausal, and HD/postmenopausal are shown in Fig. 3. An increase of signal can be observed in the series for lipid cross peaks C, D, G, and G′ in this series. The three-dimensional and 2D contour plots of the expanded spectral region (F2/F1: 3.00 ppm to 3.90 ppm), which contain the metabolites, are shown from the same participants in Fig. 4. Note the increase in signal intensity in high breast density participants (Fig. 4c and d).

Correlation of Tissue Chemistry with Breast Density

The molecules that are mobile on the MR time scale have been measured and comparisons between low and high breast density are summarized in Table 3. In women with high breast density, there is a range of metabolites that increase by a factor between 224% and 900%; the cholesterol sterol

TABLE 2. Patient Demographics According to Low and High Risk of Breast Cancer

	Low Risk (N = 53)	High Risk (N = 54)	*P*-Value
Age, mean (SD)	43.6 (12.0)	44.6 (11.0)	0.632
Menopausal status, N (%)			0.221
Premenopausal	36 (34)	28 (26)	
Postmenopausal	19 (18)	24 (22)	
Breast density, N (%)			0.026
Fatty breast	9 (8)	2 (2)	
Scattered fibroglandular tissue	24 (22)	18 (17)	
Heterogeneously dense	14 (13)	23 (22)	
Extremely dense	8 (7)	9 (8)	
BMI, mean (SD)	25.63 (5.20)	26.08 (4.84)	0.622
IBIS score, mean (SD)	10.83 (3.99)	29.35 (7.91)	<0.001

Mann–Whitney test used for mean comparison and chi-squared test for categorical variables.
N = number of subjects; SD = standard deviation; BMI = body mass index; IBIS = international breast cancer intervention study.

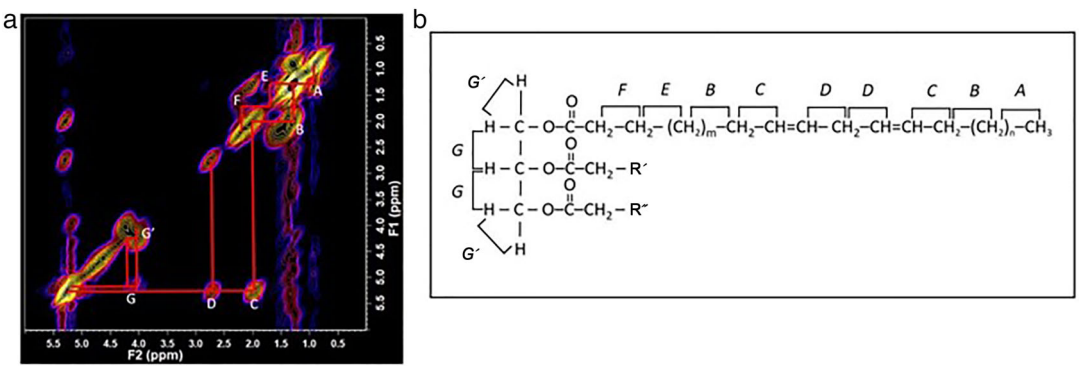

FIGURE 2: (a) Representative two-dimensional correlated spectroscopy (2D COSY) spectrum of the region F2/F1: 0.00 ppm to 6.00 ppm with the cross peaks assigned (A–G′) in a postmenopausal participant with dense breast. (b) Triglyceride molecule with associated cross peaks labeled (A–G′) identified in the spectrum. Cross peaks indicate the spin–spin coupling between adjacent hydrogen atoms. Triglyceride possesses a unique cross peak G′ at (4.10, 4.25) ppm resulting from the geminal protons of hydrogens 1 and 3 of the glycerol backbone and a cross peak denoted G at (4.25, 5.22) ppm and (4.10, 5.22) ppm, which arises from the methylene-methine coupling on the glycerol backbone.

increases by 135% and cholesterol methyl resonances by a factor of 235%.

Correlation of Tissue Chemistry with Breast Density, Menopausal Status and Risk

Tables 4 and 5 summarize the differences in tissue chemistry according to the breast density adjusted by menopausal status for both the low- and high-risk cohorts.

Participants at Low Risk

PREMENOPAUSAL PARTICIPANTS. Lipid: Compared to LD/premenopausal participants, HD/premenopausal women showed significant increase up to 308% in cholesterol methyl (0.70, 0.70) ppm, up to 154% in cholesterol sterol (0.40, 0.40) ppm, and up to 247% in the resonance from lipid ($-CH_2-CH_2-COO-$) at (1.59, 1.59) ppm. This was accompanied by an increase in triglyceride of 31% as determined by the cross peak G′ from the triglyceride backbone (Table 4).

Metabolites: The metabolites on the diagonal all significantly increased in the HD/premenopausal women, with glutamine/glutamate (3.75, 3.75) ppm increased by 900%; the composite choline, phosphocholine (3.22, 3.22) ppm 800%; taurine, glucose (3.24, 3.24) ppm 550%; *scyllo*-inositol (3.34, 3.34) ppm 520%; myo-inositol (3.27, 3.27) ppm 450%, creatine, aspartate, phosphocreatine (3.90, 3.90) ppm 320%; and the composite glycine, myo-inositol (3.50, 3.50) ppm 289% (Table 4 and Fig. 4).

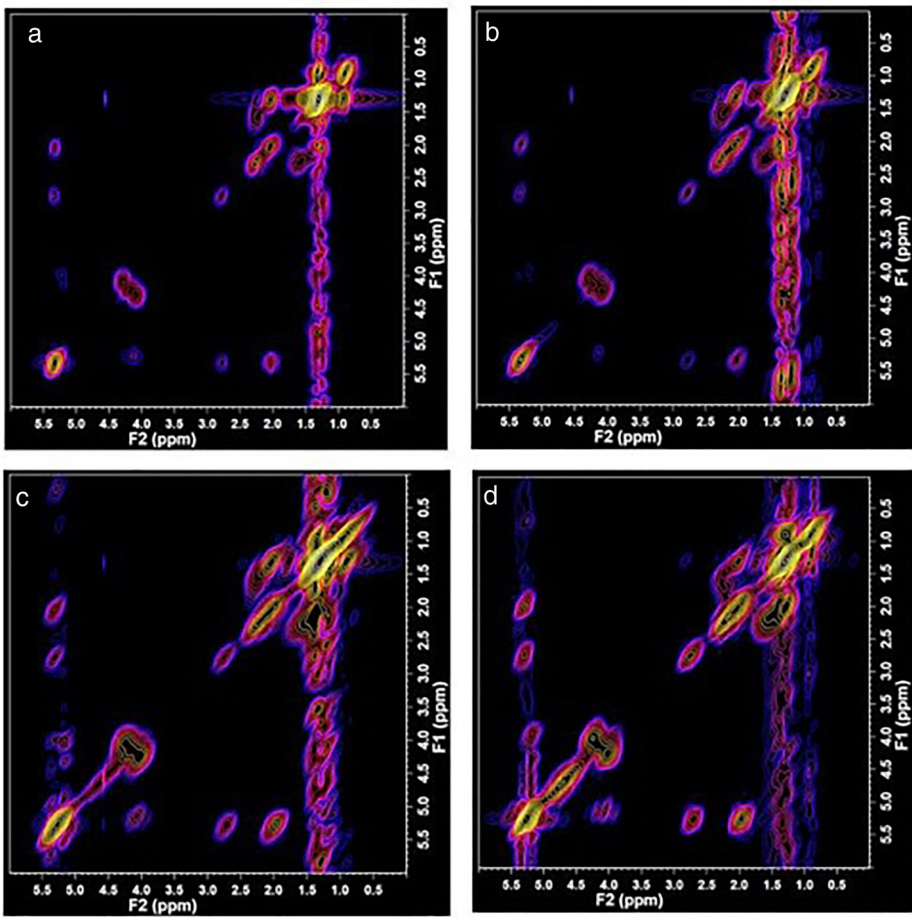

FIGURE 3: Representative two-dimensional correlated spectroscopy (2D COSY) spectra of the region F2/F1: 0.00 ppm to 6.00 ppm in participants at low risk. (a) low dense tissue and premenopausal status (30 years old), (b) low dense tissue and postmenopausal (54 years old), (c) high dense tissue and premenopausal (36 years old), and (d) high dense tissue and postmenopausal (66 years old). Note the increase in intensity for cross peaks F, D, G, and G′ across categories. See Figure 2 for assignments reference.

POSTMENOPAUSAL PARTICIPANTS. Lipid: Compared to LD/postmenopausal women, HD/postmenopausal participants recorded a significant increase in cholesterol methyl (0.70, 0.70 ppm) of 488%, cholesterol sterol (0.40, 0.40) ppm of 540%; lipid (–CH_2–CH_2–COO–) at (1.59, 1.59) ppm of 382%. Cross peak D (2.77, 5.31) ppm from the unsaturated acyl chain (=HC–CH_2–CH=CH–) increased by 160% and triglycerides by 142%, as determined by the cross peak G′. Thus, HD/postmenopausal women recorded a large increase in cholesterol and triglyceride, with a concomitant increase in unsaturated fatty acyl chains.

Metabolites: All the metabolites increased. Some increments were considerably larger than those recorded for the premenopausal group (Table 4and Fig. 4).

PAIRWISE ANALYSIS ACROSS BREAST DENSITY/MENOPAUSAL STATUS CATEGORIES. Overall, the low-risk participants showed increase in intensity for cholesterol (0.70, 0.70) ppm, cross peak F (1.59, 2.25) ppm, and cross peak G′ (4.10, 4.25) ppm and in the average volume of a number of metabolites across the four categories in the following order: LD/premenopausal, LD/postmenopausal, HD/premenopausal, and HD/postmenopausal (Fig. 5 and Table 4). Specifically, pairwise analysis showed significant differences between 1) LD/premenopausal and HD/premenopausal, 2) LD/premenopausal and HD/postmenopausal, 3) LD/postmenopausal and HD/postmenopausal, and 4) LD/postmenopausal and HD/premenopausal.

Participants at High Risk

PREMENOPAUSAL PARTICIPANTS. Lipid: In comparison with LD/premenopausal women, HD/premenopausal participants showed a 250% significant increase in the cholesterol methyl (0.70, 0.70) ppm, 72% increase in the cholesterol sterol (0.40, 0.40) ppm, and the resonance from lipid (–CH_2–CH_2–COO–) at (1.59, 1.59) ppm increased by 148% (Table 5).

Metabolites: The metabolites on the diagonal all increased significantly in the HD/premenopausal cohort, with the composite choline, phosphocholine (3.22, 3.22) ppm 1100%; taurine, glucose (3.24, 3.24) ppm 550%, glutamine/glutamate (3.75, 3.75) ppm up 450%, and leucine (3.70, 3.70) ppm 450% (Table 5).

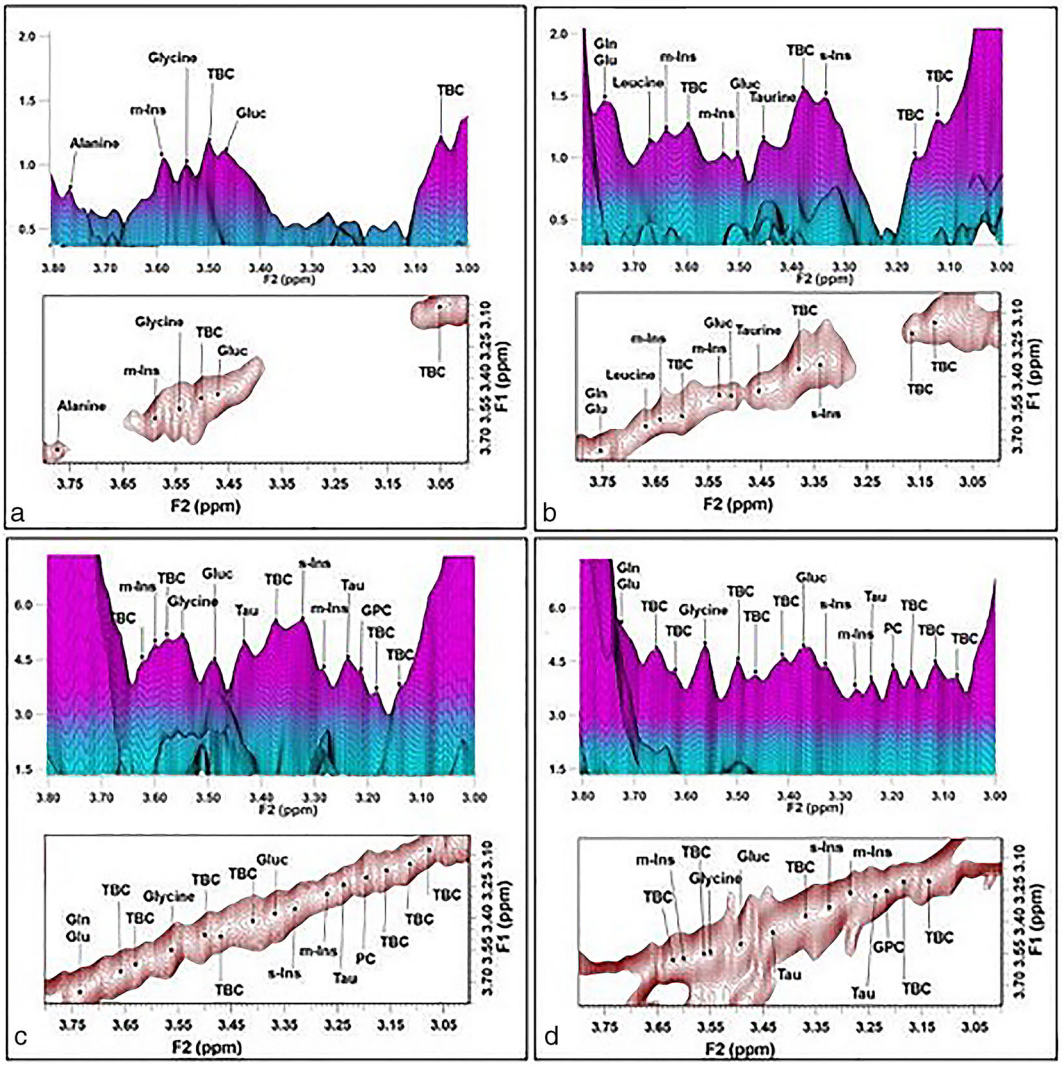

FIGURE 4: Three-dimensional (3D) and two-dimensional (2D) contour plots of the expanded region F2/F1: 3.00 ppm to 3.90 ppm (metabolite region). Same participants as in Figure 2. Standard spectral analysis utilized a level multiplier of 1.4, whereas metabolite regions utilized a level multiplier of 1.05. Representative spectra for each of the four categories: (a) low-density tissue and premenopausal status, (b) low density and postmenopausal, (c) high-density tissue and premenopausal, (d) high-density tissue and postmenopausal. 3D plots illustrate the intensity of each of the metabolites, with figures (c) and (d) having triple the intensity of (a) and (b). Contour plots demonstrate the frequencies of each diagonal resonance. Tentative assignments included m-Ins = myo-inositol; Gluc = glucose; Gln = glutamine; Glu = glutamate; s-Ins = *scyllo*-inositol; Tau = taurine; GPC = glycerophosphocholine; TBC = to be confirmed.

POSTMENOPAUSAL PARTICIPANTS. *Lipid*: HD/postmenopausal women had a slight increase in cholesterol sterol (0.40, 0.40) ppm of 47% in comparison with LD/postmenopausal women (Table 5).

Metabolites: Changes recorded for the metabolites in the HD/postmenopausal women were overall smaller than the HD/premenopausal women (Table 5).

PAIRWISE ANALYSIS ACROSS BREAST DENSITY/MENOPAUSAL STATUS CATEGORIES. The high-risk participants recorded an increase in lipid (–CH_2–CH_2–COO–) (1.59, 1.59) ppm and cross peak F (1.59, 2.25) ppm across the four categories in the following order: LD/postmenopausal, LD/premenopausal, HD/postmenopausal, and HD/premenopausal (Fig. 5 and Table 5). The pairwise analysis showed that significant differences were present between LD/premenopausal and HD/premenopausal categories and between LD/postmenopausal and HD/premenopausal.

Discussion

Increasing neutral lipid and metabolite activity was recorded with increased breast density. There were four distinct chemical profiles recorded in the in vivo 2D COSY evaluation of breast tissue in healthy women. When correlated with the risk of developing cancer, in the low-risk group, the HD/postmenopausal women showed the most active

TABLE 3. Breast Tissue Chemistry Correlated with Breast Density

Chemical Shift (F2, F1) ppm	Chemical Species	Low-Density Tissue, N = 53 (Mean)	High-Density Tissue, N = 54 (Mean)	Percentage Difference	*P*-Value
Lipids					
0.40, 0.40	Cholesterol sterol	0.00055	0.00130	*+136*	<0.001
0.70, 0.70	Cholesterol methyl	0.00109	0.00365	*+235*	<0.001
0.90, 0.90	$–CH_3$	0.08261	0.09342	*+13*	<0.001
0.90, 1.30	Lipid cross peak A	0.04267	0.03959	*−7*	<0.001
2.02, 2.02	$–CH_2–CH=CH–CH_2–$	0.04136	0.05205	*+26*	<0.001
2.02, 5.31	Lipid cross peak C	0.02212	0.02671	+21	0.363
2.25, 1.59	Lipid cross peak F	0.01812	0.02257	*+25*	<0.001
2.77, 2.77	$=CH–CH_2–CH=$	0.01182	0.01426	*+21*	0.001
2.77, 5.31	Lipid cross peak D	0.00920	0.01228	*+33*	0.043
4.10, 4.10	$–CH_2–O–(C=O)–R$	0.04065	0.04756	+17	0.147
4.10, 5.22	Lipid cross peak G	0.00736	0.00681	*−7*	0.001
5.31, 5.31	–HC=HC–	0.08738	0.10623	+22	0.695
Metabolites					
3.15, 3.15	Unassigned	0.00003	0.00022	+633	<0.001
3.19, 3.19	Unassigned	0.00001	0.00010	*+900*	<0.001
3.21, 3.21	Choline, Phosphocholine	0.00005	0.00030	*+500*	<0.001
3.22, 3.22	Choline, glycerophosphocholine	0.00001	0.00009	*+800*	<0.001
3.24, 3.24	Taurine, glucose	0.00002	0.00011	*+450*	<0.001
3.27, 3.27	Myo-inositol	0.00002	0.00010	*+400*	<0.001
3.34, 3.34	Scyllo-inositol	0.00006	0.00026	*+333*	<0.001
3.50, 3.50	Glycine, myo-inositol	0.00009	0.00030	*+233*	<0.001
3.55, 3.55	Glycine	0.00005	0.00020	*+300*	<0.001
3.70, 3.70	Leucine	0.00004	0.00023	*+475*	<0.001
3.90. 3.90	Creatine, aspartate	0.00042	0.00136	*+224*	<0.001

Mann–Whitney test used for mean comparison between categories.
F2, F1 = frequency coordinates that explain the position of each peak; N = number of subjects.

metabolic and lipid profile compared to those with low breast density who were premenopausal. In the high-risk group, the HD/premenopausal participants recorded the most chemically active metabolic profile. Interestingly, participants with low dense tissue exhibited the less active profile in both groups. These results could offer new insight about why women at high risk with dense breasts develop cancer at a younger age and might provide metabolic biomarkers of cancer development based on the lifetime risk.

The changes in breast tissue chemistry recorded in this series include neutral lipids and a range of metabolites. Each needs to be considered separately. Triglycerides and cholesterol, as neutral lipids, have a natural affinity. They create neutral droplets or domains like those found in serum lipoproteins. Articles published from the 1980s describe the behavior of these neutral lipids and their spectral characteristics.[23,24] There are two possible locations of these increased levels of neutral lipids in postmenopausal and premenopausal

TABLE 4. Comparison of Breast Tissue Chemistry According to Breast Density Adjusted for Menopausal Status in the Low-Risk Cohort

		Premenopausal (N = 36)				Postmenopausal (N = 19)			
Chemical Shift (F2, F1) ppm	Chemical Species	Low-Density, N = 19 (Mean)	High-Density, N = 17 (Mean)	*P*-Value	% Change High Density vs. Low Density	Low-Density, N = 14 (Mean)	High-Density, N = 5 (Mean)	*P*-Value	% Change High Density vs. Low Density
Lipids									
0.40, 0.40	Cholesterol sterol	0.00057	0.00145	<0.001	+154	0.00063	0.00403	0.002	+540
0.70, 0.70	Cholesterol methyl	0.00102	0.00416	<0.001	+308	0.00125	0.00735	0.005	+488
0.90, 0.90	$-CH_3$	0.08617	0.08866	0.003	+3	0.08668	0.17348	0.007	+100
0.90, 1.30	Cross peak A	0.04289	0.03775	0.006	−12	0.04199	0.03650	0.070	−13
1.59, 1.59	$-CH_2-CH_2-COO-$	0.01789	0.06216	<0.001	+247	0.01823	0.08788	0.001	+382
2.02, 2.02	$-CH_2-HC=HC-CH_2-$	0.04327	0.05088	<0.001	+18	0.04393	0.10904	0.001	+148
2.02, 5.31	Cross peak C	0.01747	0.01564	0.876	−10	0.01724	0.04320	0.087	+151
2.25, 2.25	$-CH_2-COO-$	0.02991	0.03244	0.011	+8	0.02969	0.06695	0.005	+125
2.25, 1.59	Cross peak F	0.03168	0.04118	0.001	+30	0.03168	0.07422	0.001	+134
2.77, 2.77	$=HC-CH_2-HC=$	0.01295	0.01434	0.006	+11	0.01283	0.03343	0.001	+161
2.77, 5.31	Cross peak D	0.00789	0.00809	0.594	+3	0.00761	0.01976	0.026	+160
4.25, 5.22	Cross peak G	0.00834	0.00545	0.016	−3	0.00754	0.01292	0.156	+71
4.10, 4.25	Cross peak G′	0.06470	0.08488	0.016	+31	0.07442	0.18042	0.003	+142
5.31, 5.31	–CH=HC–	0.09507	0.09536	0.363	+0	0.09263	0.31415	0.001	+207
Metabolites									
3.03, 3.03	Creatine	0.00013	0.00051	<0.001	+292	0.00015	0.00129	0.001	+760
3.15, 3.15	Unassigned	0.00003	0.00022	<0.001	+633	0.00004	0.00034	0.003	+750
3.19, 3.19	Unassigned	0.00001	0.00011	<0.001	+1000	0.00002	0.00016	0.001	+700
3.22, 3.22	Choline, phosphocholine	0.00001	0.00009	<0.001	+800	0.00002	0.00015	0.005	+650
3.24, 3.24	Taurine, glucose	0.00002	0.00013	<0.001	+550	0.00003	0.00020	0.005	+567
3.27, 3.27	Myo-inositol	0.00002	0.00011	<0.001	+450	0.00002	0.00021	0.003	+950

TABLE 4. Continued

Chemical Shift (F2, F1) ppm	Chemical Species	Premenopausal (N = 36) Low-Density, N = 19 (Mean)	Premenopausal (N = 36) High-Density, N = 17 (Mean)	Premenopausal (N = 36) *P*-Value	Premenopausal (N = 36) % Change High Density vs. Low Density	Postmenopausal (N = 19) Low-Density, N = 14 (Mean)	Postmenopausal (N = 19) High-Density, N = 5 (Mean)	Postmenopausal (N = 19) *P*-Value	Postmenopausal (N = 19) % Change High Density vs. Low Density
3.34, 3.34	*Scyllo*-inositol	0.00005	0.00031	<0.001	+520	0.00007	0.00053	0.002	+657
3.42, 3.42	Taurine	0.00006	0.00027	<0.001	+350	0.00007	0.00046	0.010	+557
3.50, 3.50	Glycine, myo-inositol	0.00009	0.00035	<0.001	+289	0.00010	0.00064	0.005	+540
3.55, 3.55	Glycine	0.00006	0.00022	<0.001	+267	0.00006	0.00041	0.001	+583
3.61, 3.61	Myo-inositol	0.00009	0.00042	<0.001	+367	0.00009	0.00066	0.001	+633
3.64, 3.64	Myo-inositol	0.00003	0.00015	<0.001	+400	0.00003	0.00021	0.010	+600
3.70, 3.70	Leucine	0.00003	0.00032	<0.001	+967	0.00004	0.00030	0.014	+650
3.75, 3.75	Glutamine, glutamate	0.00003	0.00030	<0.001	+900	0.00005	0.00033	0.034	+560
3.78, 3.78	Alanine	0.00004	0.00034	<0.001	+750	0.00006	0.00045	0.014	+650
3.90, 3.90	Creatine, aspartate, phosphocreatine	0.00041	0.00172	<0.001	+320	0.00052	0.00278	0.005	+435

Mann–Whitney test used for mean comparison between categories.
F2, F1 = frequency coordinates that explain the position of each peak; N = number of subjects.

TABLE 5. Comparison of Breast Tissue Biochemistry According to Breast Density Adjusted for Menopausal Status in the High-Risk Cohort

		Premenopausal (N = 28)				Postmenopausal (N = 24)			
Chemical Shift (F2, F1) ppm	Chemical Species	Low Density, N = 9 (Mean)	High Density, N = 19 (Mean)	*P*-Value	% Change High Density vs. Low Density	Low Density, N = 11 (Mean)	High Density, N = 13 (Mean)	*P*-Value	% Change High Density vs. Low Density
Lipids									
0.40, 0.40	Cholesterol sterol	0.00050	0.00086	0.016	+72	0.00047	0.00069	0.001	+47
0.70, 0.70	Cholesterol methyl	0.00101	0.00353	<0.001	+250	0.00108	0.00175	0.134	+62
0.90, 0.90	$-CH_3$	0.07757	0.08759	0.105	+13	0.07543	0.07736	0.531	+3
0.90, 1.30	Cross peak A	0.04392	0.03947	0.005	−10	0.04213	0.04335	0.776	+3
1.59, 1.59	$-CH_2-CH_2-COO-$	0.01678	0.04160	0.001	+148	0.01925	0.02630	0.331	+37
2.02, 2.02	$-CH_2-HC=HC-CH_2-$	0.03938	0.04639	0.016	+18	0.03640	0.03996	0.252	+10
2.02, 5.31	Cross peak C	0.01494	0.01385	0.410	−7	0.01347	0.01347	0.424	+0
2.25, 2.25	$-CH_2-COO-$	0.02600	0.02972	0.037	+14	0.02533	0.02678	0.569	+6
2.25, 1.59	Cross peak F	0.02797	0.03441	0.033	+23	0.02641	0.03074	0.119	+16
2.77, 2.77	$=HC-CH_2-HC=$	0.01295	0.01434	0.735	+11	0.00945	0.01133	0.106	+20
2.77, 5.31	Cross peak D	0.00645	0.00607	0.438	−6	0.00554	0.00612	0.608	+10
4.25, 5.22	Cross peak G	0.00663	0.00740	0.076	+17	0.00605	0.00537	0.277	−11
4.10, 4.25	Cross peak G′	0.05874	0.09006	0.076	+53	0.05281	0.05884	0.776	+11
5.31, 5.31	$-CH=HC-$	0.07947	0.08077	0.699	+2	0.07388	0.07767	0.494	+5
Metabolites									
3.03, 3.03	Creatine	0.00009	0.00058	<0.001	+544	0.00013	0.00023	0.063	+77
3.15, 3.15	Unassigned	0.00003	0.00029	0.001	+867	0.00002	0.00007	0.011	+250
3.19, 3.19	Unassigned	0.00001	0.00012	<0.001	+1100	0.00001	0.00003	0.041	+200
3.22, 3.22	Choline, phosphocholine	0.00001	0.00012	<0.001	+1100	0.00001	0.00003	0.082	+200
3.24, 3.24	Taurine, glucose	0.00002	0.00013	<0.001	+550	0.00002	0.00004	0.002	+100
3.27, 3.27	Myo-inositol	0.00002	0.00011	0.005	+450	0.00002	0.00003	0.022	+50

TABLE 5. Continued

Chemical Shift (F2, F1) ppm	Chemical Species	Premenopausal (N = 28)				Postmenopausal (N = 24)			
		Low Density, N = 9 (Mean)	High Density, N = 19 (Mean)	*P*-Value	% Change High Density vs. Low Density	Low Density, N = 11 (Mean)	High Density, N = 13 (Mean)	*P*-Value	% Change High Density vs. Low Density
3.34, 3.34	*Scyllo*-inositol	0.00005	0.00027	0.001	+440	0.00005	0.00010	0.228	+100
3.42, 3.42	Taurine	0.00006	0.00022	0.001	+267	0.00005	0.00009	0.167	+80
3.50, 3.50	Glycine, myo-inositol	0.00008	0.00029	<0.001	+263	0.00008	0.00009	0.093	+13
3.55, 3.55	Glycine	0.00005	0.00022	0.002	+340	0.00005	0.00007	0.331	+40
3.61, 3.61	Myo-inositol	0.00009	0.00040	0.007	+344	0.00007	0.00012	0.063	+71
3.64, 3.64	Myo-inositol	0.00003	0.00013	0.007	+333	0.00002	0.00004	0.030	+100
3.70, 3.70	Leucine	0.00004	0.00022	0.001	+450	0.00003	0.00007	0.055	+133
3.75, 3.75	Glutamine, glutamate	0.00004	0.00022	0.002	+450	0.00004	0.00008	0.072	+100
3.78, 3.78	Alanine	0.00005	0.00022	0.002	+340	0.00004	0.00010	0.055	+150
3.90, 3.90	Creatine, aspartate, phosphocreatine	0.00038	0.00118	<0.001	+211	0.00034	0.00059	0.134	+74

Mann–Whitney test used for mean comparison between categories.
F2, F1 = Frequency coordinates that explain the position of each peak; N = number of subjects.

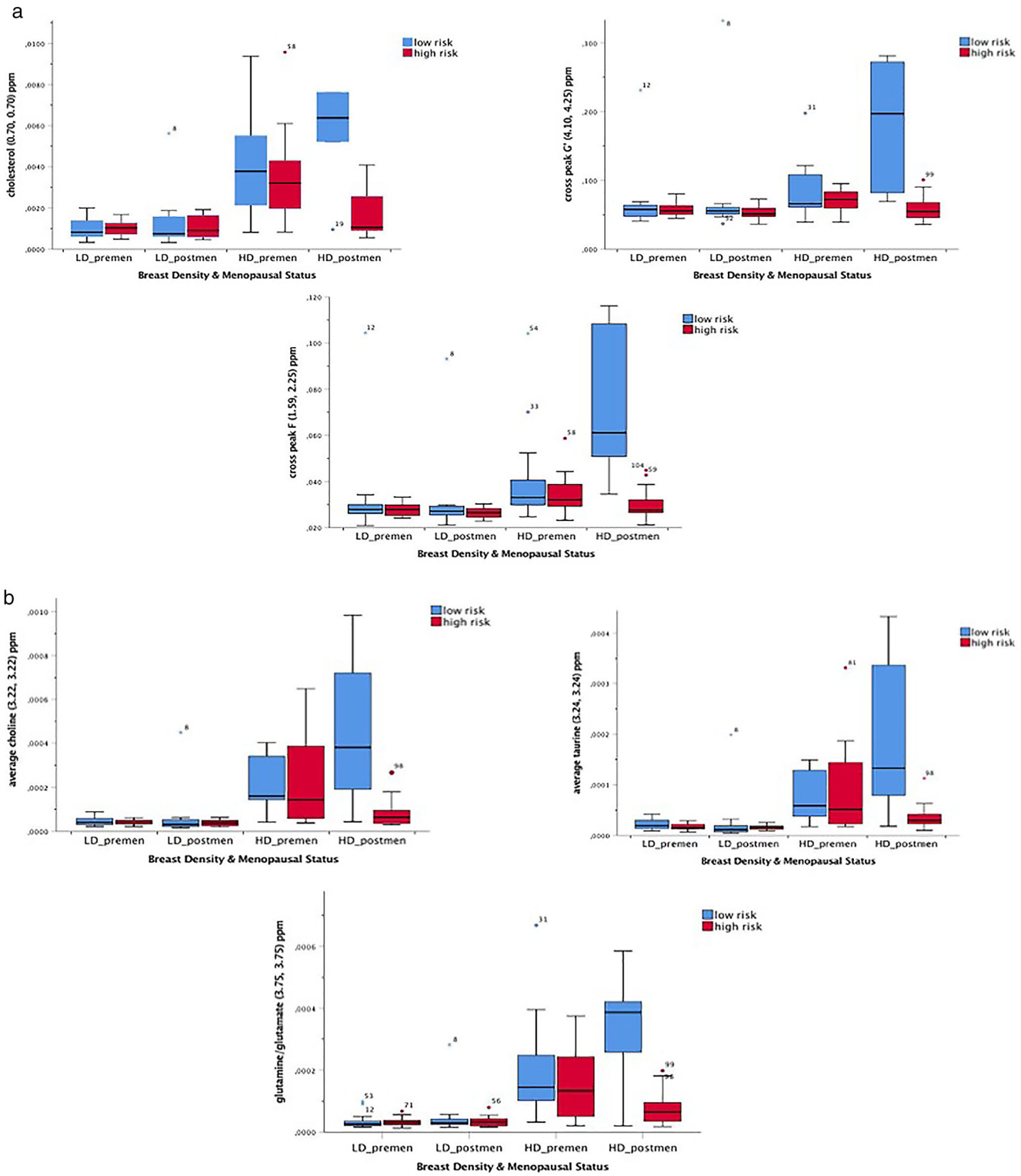

FIGURE 5: (a) Clustered box plots display the median volumes and interquartile ranges of cholesterol, triglyceride backbone/cross peak G′, and cross peak F in low- and high-risk groups across the four categories identified based on breast density and menopausal status. (b) Clustered box plots display the median volumes and interquartile ranges of choline/phosphocholine, taurine/glucose and glutamine/glutamate. Note that the least chemically active categories corresponded to low-density breasts, both for premenopausal and postmenopausal participants, regardless of risk.

dense breast tissue. The first is in the cytoplasm where they would provide the lipid pool for rapid doubling of cells when needed. The second is in the plasma membranes of activated or stimulated cells, such as macrophages or other inflammatory cells. A model was proposed whereby neutral lipid domains are intercalated with the bilayer lipid of the plasma

membrane of activated, stimulated, or transformed cells.[25] This model was contentious[26] initially but verified many years later.[27] The resonance at 0.70 ppm has previously been assigned to cholesterol C18[23] and shown to have rapid molecular motion. As the triglyceride and cholesterol ester levels increase, the cholesterol becomes more mobile and can be measured.

King et al[28] used 2D COSY to study murine macrophages and found that proliferation is not a prerequisite for acquisition of an "activated" high-resolution spectrum in cell models. There is evidence that dense breast tissue in postmenopausal women is associated with a pro-inflammatory microenvironment including cytokines and a significantly increased number of inflammatory cells.[29] Additionally, increased levels of pro-inflammatory cytokines have been shown to stimulate triglyceride synthesis, cholesterol accumulation and de novo lipogenesis[30] which would explain our findings in the low-risk group, with postmenopausal women with dense breasts exhibiting the highest increase in triglycerides and cholesterol. Likewise, high mammographic density has been reported to be associated with protumor inflammation.[31] This pro-inflammatory microenvironment would underpin the active chemical profiles we identified in dense breasts. Importantly, the highest chemical activity shifts from postmenopausal to premenopausal women based on whether they pertain to the low-risk or to the high-risk group, respectively. This is an important observation as familial breast cancer is known to be of early onset.[32] Our results in the low-risk cohort are in line with those reported by Advani et al[33] on a large series of women aged 65 or older who underwent screening mammography. They reported that breast density was associated with increased breast cancer risk among women aged 65 years to 74 years regardless of BMI.

The gradual increase in metabolites through the series include glucose and taurine, choline, myo-inositol, and glutamine/glutamate. Morris et al[34] reported a decrease in glucose metabolism in HD tissue collagen matrices and found an enhanced contribution of glutamine as a fuel source in these matrices. Similarly, others reported that glucose metabolism significantly increased in HD tissue, but was not affected by menopausal status.[35]

We recorded a steady increase in myo-inositol through this series. Myo-inositol has been shown to modulate inflammatory, oxidative, endocrine, and metabolic pathways.[36] In parallel, taurine has been reported to be an antioxidant that exerts antineoplastic effects through downregulation of angiogenesis and suppressing cell proliferation.[37] Thus, some of these changes recorded in the healthy breast are likely to be part of protective mechanisms. This requires further evaluation.

Limitations

Firstly, the data from premenopausal women were taken at the end of the follicular phase of their menstrual cycle. This may have an impact on the results as the lipid composition may change slightly during the menstrual cycle.[38] Secondly, our results show an increase over all volumes of metabolites in dense breasts compared to nondense breasts. Note should be made that some of these volumes are composites of metabolites, which makes it difficult to confirm whether or not some metabolites of these composites could be decreased in relation to others. Lastly, it is likely that some resonances on the diagonal are composites. With future improvements in scanner capabilities, and increases in signal-to-noise ratio, they may be recorded with their associated cross peaks and thus assigned unambiguously.

Conclusion

Four distinct chemical profiles were identified in breast tissue based on breast density and menopausal status in healthy participants at low risk and high risk of breast cancer. Gradual increase in neutral lipid content and metabolites was noted in both risk groups across categories in different order. In women at low risk, the HD postmenopausal category exhibited the highest metabolic activity, while women at high risk with no known mutation exhibited the highest lipid content and metabolic activity in the HD premenopausal category.

In summary, our results indicate that high breast density is associated with a significantly more active tissue chemistry and might offer an explanation as to why postmenopausal women with dense breast in low-risk cohorts and premenopausal women with HD breast in high-risk cohorts are more likely to develop cancer.

From a clinical perspective, the capacity to monitor these changes in healthy breast tissue noninvasively by adding a 19-minute sequence on to a breast MR protocol may provide valuable biochemical information of metabolism in the breast tissue both in low-risk and high-risk cohorts. Although the metabolic profiles described need to be reproduced in larger series, they might be relevant for risk classification tasks.

Acknowledgments

The authors thank Juan Ramón Sabaté, César Garrido, Lidón Pages, Xavier Bargalló, and Sergi Ganau from Hospital Clinic de Barcelona; Randell Brown, Timothy King, and Jillian Borthwick from St Andrew's Hospital in Adelaide for their assistance in participant recruitment and data acquisition.

Open access publishing facilitated by Queensland University of Technology, as part of the Wiley - Queensland University of Technology agreement via the Council of Australian University Librarians.

References

1. McCormack VA, dos Santos SI. Breast density and parenchymal patterns as markers of breast cancer risk: A meta-analysis. Cancer Epidemiol Biomarkers Prev 2006;15:1159-1169.
2. Boyd NF, Lockwood GA, Byng JW, Tritchler DL, Yaffe MJ. Mammographic densities and breast cancer risk. Cancer Epidemiol Biomarkers Prev 1998;7:1133-1144.
3. Duffy SW, Morrish OWE, Allgood PC, et al. Mammographic density and breast cancer risk in breast screening assessment cases and women with a family history of breast cancer. Eur J Cancer 2018;88: 48-56.
4. Boyd NF, Guo H, Martin LJ, et al. Mammographic density and the risk and detection of breast cancer. N Engl J Med 2007;356:227-236.
5. Veronesi U, Boyle P, Goldhirsch A, Orecchia R, Viale G. Breast cancer. Lancet 2005;365:1727-1741.
6. D'Orsi CJ, Sickles EA, Mendelson EB, Morris EA. *ACR BI-RADS atlas, breast imaging reporting and data system*. Reston, Virginia: American College of Radiology; 2003.
7. Ironside A, Jones L. Stromal characteristics may hold the key to mammographic density: The evidence to date. Oncotarget 2016;7:31550-31562.
8. Lin SJ, Cawson J, Hill P, et al. Image-guided sampling reveals increased stroma and lower glandular complexity in mammographically dense breast tissue. Breast Cancer Res Treat 2011;128:505-516.
9. Guo Y-P, Martin LJ, Hanna W, et al. Growth factors and stromal matrix proteins associated with mammographic densities. Cancer Epidemiol Biomarkers Prev 2001;10:243-248.
10. Wang J, Wang MY, Kuo WH, Chen KL, Shih TT. Proton MR spectroscopy of normal breasts: Association of risk factors for breast cancer with water and lipid composition of the breast. Magn Reson Imaging 2016; 34:524-528.
11. Ramadan S, Arm J, Silcock J, et al. Lipid and metabolite deregulation in the breast tissue of women carrying BRCA1 and BRCA2 genetic mutations. Radiology 2015;275:675-682.
12. Thomas MA, Lipnick S, Velan SS, et al. Investigation of breast cancer using two-dimensional MRS. NMR Biomed 2009;22:77-91.
13. Mackinnon WB, May GL, Mountford CE. Esterified cholesterol and triglycerides are present in plasma membranes of Chinese hamster ovary cells. Eur J Biochem/FEBS 1992;205:827-839.
14. Mackinnon WB, Dyne M, Hancock R, Mountford CE, Grant AJ, Russell P. Malignancy-related characteristics of wild type and drug-resistant Chinese hamster ovary cells. Pathology 1993;25:268-276.
15. Mackinnon WB, Huschtscha L, Dent K, Hancock R, Paraskeva C, Mountford CE. Correlation of cellular differentiation in human colorectal carcinoma and adenoma cell lines with metabolite profiles determined by 1H magnetic resonance spectroscopy. Int J Cancer 1994;59: 248-261.
16. Glunde K, Bhujwalla ZM, Ronen SM. Choline metabolism in malignant transformation. Nat Rev Cancer 2011;11:835-848.
17. Mulsow J, Lee J, Dempsey C, Rothwell J, Geraghty JG. Establishing a family risk assessment clinic for breast cancer. Breast J 2009;15(Suppl 1):S33-S38.
18. Tyrer J, Duffy SW, Cuzick J. A breast cancer prediction model incorporating familial and personal risk factors. Stat Med 2004;23:1111-1130.
19. Saslow D, Boetes C, Burke W, et al. American Cancer Society guidelines for breast screening with MRI as an adjunct to mammography. CA Cancer J Clin 2007;57:75-89.
20. Mountford C, Ramadan S, Stanwell P, Malycha P. Proton MRS of the breast in the clinical setting. NMR Biomed 2009;22:54-64.
21. Ogg RJ, Kingsley PB, Taylor JS. WET, a T1- and B1-insensitive water-suppression method for in vivo localized 1H NMR spectroscopy. J Magn Reson B 1994;104:1-10.
22. Sitter B, Sonnewald U, Spraul M, Fjosne HE, Gribbestad IS. High-resolution magic angle spinning MRS of breast cancer tissue. NMR Biomed 2002;15:327-337.
23. Hamilton JA, Morrisett JD. Nuclear magnetic resonance studies of lipoproteins. Methods Enzymol 1986;128:472-515.
24. Avila EM, Hamilton JA, Harmony HAK, Allerhand A, Cordes EH. Natural abundance ^{13}C nuclear magnetic resonance studies of human plasma high density lipoproteins. J Biol Chem 1978;253:3983-3987.
25. Mountford CE, Wright LC. Organization of lipids in the plasma membranes of malignant and stimulated cells: A new model. Trends Biochem Sci 1988;13:172-177.
26. Hakumäki JM, Kauppinen RA. 1H NMR visible lipids in the life and death of cells. Trends Biochem Sci 2000;25:357-362.
27. Khandelia H, Duelund L, Pakkanen KI, Ipsen JH. Triglyceride blisters in lipid bilayers: Implications for lipid droplet biogenesis and the mobile lipid signal in cancer cell membranes. PLoS One 2010;5:e12811.
28. King NJC, Ward MH, Holmes KT. Magnetic resonance studies of murine macrophages: Proliferation is not a prerequisite for acquisition of an 'activated' high resolution spectrum. FEBS Lett 1991;287:97-101.
29. Abrahamsson A, Rzepecka A, Romu T, et al. Dense breast tissue in postmenopausal women is associated with a pro-inflammatory microenvironment *in vivo*. Oncoimmunology 2016;5:e1229723.
30. Shi J, Fan J, Su Q, Yang Z. Cytokines and abnormal glucose and lipid metabolism. Front Endocrinol 2019;10:703.
31. Huo CW, Hill P, Chew G, et al. High mammographic density in women is associated with protumor inflammation. Breast C Res 2018;20: 92-108.
32. Brandt A, Bermejo JL, Sundquist J, Hemminki K. Age of onset in familial breast cancer as background data for medical surveillance. Br J Cancer 2010;102:42-47.
33. Advani SM, Zhu W, Demb J, et al. Association of breast density with breast cancer risk among women aged 65 years or older by age group and body mass index. JAMA Netw Open 2021;4(8):e2122810. https://doi.org/10.1001/jamanetworkopen.2021.22810.
34. Morris BA, Burkel B, Ponik SM, et al. Collagen matrix density drives the metabolic shift in breast cancer cells. EBioMedicine 2016;13:146-156.
35. Mavi A, Cermik TF, Urhan M, et al. The effect of age, menopausal state, and breast density on ^{18}F-FDG uptake in normal glandular breast tissue. J Nucl Med 2010;51:347-352.
36. Pasta V, Gullo G, Giuliani A, et al. An association of boswellia, betaine and myo-inositol (Eumastós) in the treatment of mammographic breast density: A randomized, double-blind study. Eur Rev Med Pharmacol Sci 2015;19:4419-4426.
37. El Agouza IM, Eissa SS, El Houseini MM, El-Nashar DE, Abd El Hamed OM. Taurine: A novel tumor marker for enhanced detection of breast cancer among female patients. Angiogenesis 2011;14:321-330.
38. Dzendrowskyj TE, Noyszewski JB, Bolinger L. Lipid composition changes in normal breast throughout the menstrual cycle. MAGMA 1997;5:105-110.